THE JOURNAL OF PHYSICAL CHEMISTRY A

 VOLUME 110, NUMBER 15, APRIL 20, 2006

FEATURE ARTICLE

Prying Apart a Water Molecule with Anionic H-Bonding: A Comparative Spectroscopic Study of the $X^-\cdot H_2O$ (X = OH, O, F, Cl, and Br) Binary Complexes in the 600−3800 cm^{-1} Region

Joseph R. Roscioli, Eric G. Diken, and Mark A. Johnson*
Sterling Chemistry Laboratories, Yale University, P.O. Box 208107, New Haven, Connecticut 06520

Samantha Horvath and Anne B. McCoy*
Department of Chemistry, The Ohio State University, Columbus, Ohio 43210

Received: October 20, 2005; In Final Form: February 8, 2006

A detailed picture of the structural distortions suffered by a water molecule in direct contact with small inorganic anions (e.g., X = halide) is emerging from a series of recent vibrational spectroscopy studies of the gas-phase $X^-\cdot H_2O$ binary complexes. The extended spectral coverage (600−3800 cm^{-1}) presently available with tabletop laser systems, when combined with versatile argon "messenger" techniques for acquiring action spectra of cold complexes, now provides a comprehensive survey of how the interaction evolves from an ion−solvent configuration into a three-center, two-electron covalent bond as the proton affinity of the anion increases. We focus on the behavior of H_2O in the $X^-\cdot H_2O$ (X = Br, Cl, F, O, and OH) complexes, which all adopt asymmetric structures where one hydrogen atom is H-bonded to the ion while the other is free. The positions and intensities of the bands clearly reveal the mechanical consequences of both (zero-point) vibrationally averaged and infrared photoinduced excess charge delocalization mediated by intracluster proton transfer ($X^-\cdot H_2O \rightarrow HX\cdot OH^-$). The fundamentals of the shared proton stretch become quite intense, for example, and exhibit extreme red-shifts as the intracluster proton-transfer process becomes available, first in the vibrationally excited states ($F^-\cdot H_2O$) and then finally at the zero-point level ($OH^-\cdot H_2O$). In the latter case, the loss of the water molecule's independent character is confirmed through the disappearance of the ∼1600 cm^{-1} HOH intramolecular bending transition and the dramatic (>3000 cm^{-1}) red-shift of the shared proton stretch. An unexpected manifestation of vibrationally mediated charge transfer is also observed in the low frequency region, where the $2 \leftarrow 0$ overtones of the out-of-plane frustrated rotation of the water are remarkably intense in the $Cl^-\cdot H_2O$ and $Br^-\cdot H_2O$ spectra. This effect is traced to changes in the charge distribution along the $X^-\cdot O$ axis as the shared proton is displaced perpendicular to it, reducing the charge transfer character of the H-bonding interaction and giving rise to a large quadratic contribution to the dipole moment component that is parallel to the bond axis. Thus, all of these systems are found to exhibit distinct spectral characteristics that can be directly traced to the crucial role of vibrationally mediated charge redistribution within the complex.

I. Introduction

The isolated monohydrates of simple atomic and molecular anions, $X^-\cdot H_2O$ (X = halogen, Cu, O_2, RCO_2, etc.), have been subjected to intense study as model systems with which to explore the intramolecular distortions at play in the anionic H-bond.[1−16] A key development driving the present resurgence of interest in these systems is that predictions of the $X^-\cdot H_2O$ structures and vibrational energy level patterns obtained using the most advanced theoretical treatments[5,6,8,12,15] can be chal-

* To whom correspondence should be addressed. E-mail: mark.johnson@yale.edu (M.A.J.); mccoy@chemistry.ohio-state.edu (A.B.M.).

10.1021/jp056022v CCC: $33.50
Published on Web 03/25/2006

Joseph R. Roscioli received a B.Phil. in Chemistry and Astrophysics and a B.A. in History and Philosophy of Science from the University of Pittsburgh in 2003, where he also studied high resolution electronic spectroscopy of biologically relevant molecules. He is currently pursuing his Ph.D. at Yale University, with particular focus on water solvation in elementary anionic systems using infrared and photoelectron spectroscopy.

Eric G. Diken received his B.S. degree from Rutgers University in 2001, where he worked with E. W. Castner, Jr., studying local friction and dynamics in aqueous polymer solutions. He then moved to Yale University where he studied fundamental chemical reactions and the cooperativity of hydrogen bonds in solvated clusters, under the supervision of M. A. Johnson. He earned his Ph.D. in 2005 and is now applying his technical skills as a scientist for Smith's Detection.

Mark A. Johnson received his B.S. degree in Chemistry from the University of California, Berkeley, in 1977 and his Ph.D. from Stanford University in 1983. He then became a postdoctoral associate at J.I.L.A. and the University of Colorado, Boulder, working for W. C. Lineberger. In 1985, he joined the Department of Chemistry at Yale University, where he is currently the Arthur T. Kemp Professor of Chemistry. His research interests focus on solute−solvent interactions and how they affect the structure and outcomes of reactive encounters.

Samantha Horvath received her bachelor's degree in Chemistry from the University of Tampa in Tampa, Florida, in 2004. She received an REU fellowship to the University of Virginia before beginning her graduate school career at the Ohio State University, where she is currently working toward her Ph.D. with Dr. Anne McCoy. Her research focuses on the potential energy surfaces and spectroscopy of hydrogen-bonded complexes.

Anne B. McCoy received her B.S. degree in Chemistry from Haverford College in 1987 and her Ph.D. at the University of Wisconsin, Madison, in 1992. She was a Golda Meir Postdoctoral Fellow at the Hebrew University in Jerusalem and University of California, Irvine, working with Benny Gerber. She is currently a professor in the Department of Chemistry at the Ohio State University. Research in her group focuses on the spectroscopy and dynamics of weakly bound complexes as well as understanding spectral signatures of large amplitude motions and hydrogen bonding.

lenged directly by the experimental data that is now available through the application of argon predissociation spectroscopy.[11] In this paper, we exploit recent breakthroughs in nonlinear optics that enable broad (600−3800 cm^{-1}) spectral coverage[17] to record the infrared band patterns for the X = OH, O, F, Cl, and Br series of monohydrates. These species were selected to establish the spectroscopic signatures that encode the transition of the anionic H-bond from a relatively weak ion−molecule interaction to the very strong binding regime where one proton is best regarded as being engaged in a three-center, two-electron covalent bond reminiscent of that adopted by the symmetrical XHX^- triatomic anions.[18,19]

The basic bonding motif at play in the $X^-\cdot H_2O$ systems involving monatomic anions[2,4,8,11,20,21] is the single ionic H-bond (SIHB) arrangement, where one proton is strongly shared and the other nonbonded or "free" OH plays the role of a spectator, as indicated by the calculated $X^-\cdot H_2O$ structures (MP2/aug-cc-pVDZ level of theory)[22] presented in Figure 1. The SIHB motif is immediately apparent in the $X^-\cdot H_2O$ vibrational spectra, as the free OH stretch (ν_f) typically oscillates near the centroid of the two OH stretches in the isolated water molecule (~3707 cm^{-1})[23] and is largely insensitive to the anion, whereas the ionic H-bonded OH stretch (ν_{IHB}) is dramatically red-shifted in a manner strongly correlated with the proton affinity of the anion.[11] As an indication of the range spanned by these

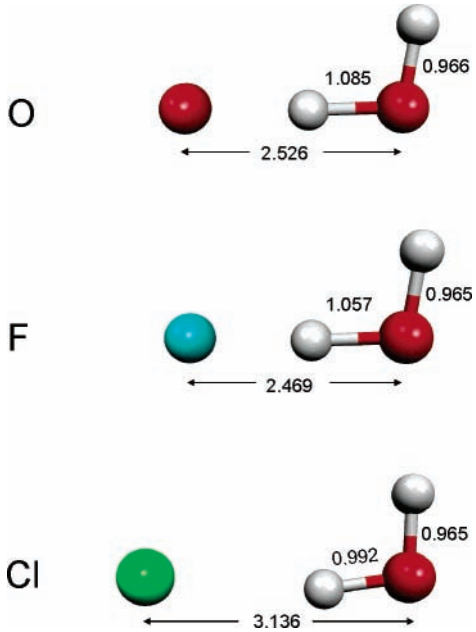

Figure 1. Calculated structures for the $X^-\cdot H_2O$ (X = O, F, and Cl) binary complexes, with structural parameters indicated in angstroms (MP2/aug-cc-pVDZ level of theory).

TABLE 1: Theoretical (MP2/aug-cc-pVDZ) Proton-Transfer Parameters [$\rho_{PT} = (R_{O-H} - R^\circ_{OH}) - (R_{X-H} - R^\circ_{XH})$] for the $X^-\cdot H_2O$ System[24,25]

X^-	ρ_{PT} (Å)
Br	−0.933
Cl	−0.857
F	−0.404
O	−0.351
OH	−0.333

complexes, it is informative to index the extent of proton transfer by the parameter ρ_{PT}, defined as

$$\rho_{PT} = (R_{O-H} - R^\circ_{OH}) - (R_{X-H} - R^\circ_{XH}) \quad (1)$$

where $R_i - R_i^\circ$ indicates the difference between bond distances in the minimum energy $X^-\cdot H_2O$ structures and the respective values in the isolated H_2O and HX molecules.[24,25] This index is thus most negative when the water molecule is largely intact and passes through zero when both bonds are equally distorted relative to their neutral parent molecules. The values extracted from the calculated $X^-\cdot H_2O$ structures (Figure 1) are included in Table 1, where the negative values adopted by this series explore a significant range of behavior for essentially X^- (as opposed to hydroxide)-based complexes. Note that the most strongly basic O^- and OH^- ions yield the least negative ρ_{PT} values in the neighborhood of −0.3.

The preference for the SIHB structural arrangement and the strong red-shifts of the ν_{IHB} stretches can both be viewed as consequences of the relatively low-lying endothermic intracluster proton-transfer process:[7]

$$X^-\cdot H_2O \rightarrow HX\cdot OH^- \quad (2)$$

which is the cluster analogue of the Brønsted base hydrolysis reaction. In this context, the ion-dependent red-shift of the shared proton vibration can be attributed to the depression of the potential curve describing the motion of the H atom parallel to the bond axis, where the product channel $HX\cdot OH^-$ species is manifested as a "shelf" whose height varies according to the X^- proton affinity. To quantify this effect, Figure 2 compares

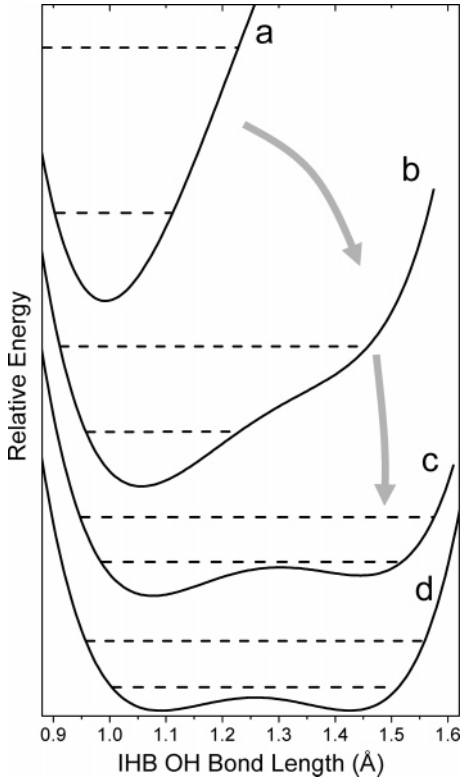

Figure 2. Potential energy surfaces for the intracluster proton-transfer coordinate of the (a) $Cl^-\cdot H_2O$, (b) $F^-\cdot H_2O$, (c) $O^-\cdot H_2O$, and (d) $OH^-\cdot H_2O$ binary complexes, presented from top to bottom in increasing order of anion basicity. Calculations (at the MP2/aug-cc-pVDZ level of theory) were carried out by fixing the separation between the heavy atoms at the equilibrium geometry and increasing the OH bond length of the shared proton while allowing all other degrees of freedom to relax. Dashed lines indicate the first two vibrational levels of the shared proton motion, extracted from numerical solutions to the one-dimensional Schrödinger equation using these potentials. The gray arrows emphasize the increasing importance of the shelf in the potential arising from the $OH^-\cdot HX$ configuration. Note that the Cl^- complex is confined to more charge-localized configurations in both the $v = 0$ and 1 levels, while first the upper (F^-) and then the ground vibrational levels (OH^-) become delocalized between the heavy atoms as anion basicity increases.

the calculated potentials (MP2/aug-cc-pVDZ level of theory) for the X = Cl, F, O, and OH complexes, which were generated by scanning the shared proton position with the heavy atoms held fixed at their separations in the minimum energy structures. The free OH group is allowed to adiabatically relax at each step of the calculation.

The shapes of the curves in Figure 2 reveal that this series of complexes should indeed explore the critical range where intracluster proton transfer (and hence excess charge delocalization over the heavy atoms) becomes increasingly important. For example, in $Cl^-\cdot H_2O$, the potential is well described with a typical anharmonic (e.g., Morse) form up to the first ν_{IHB} vibrational level, and the charge is therefore expected to be mostly localized on the halide in both the ground and the first excited vibrational levels. In $F^-\cdot H_2O$, on the other hand, calculations indicate that, although the zero-point level is charge-localized, the first vibrational level occurs over the shelf,[26] so that vibrational excitation along this coordinate should drive charge delocalization (i.e., $F^-\cdot H_2O \rightarrow FH\cdot OH^-$). Note that the resulting extreme change in the electronic wave function as the shared proton passes over the shelf naturally accounts for the anomalously large oscillator strength of the ν_{IHB} bands in the more strongly-bound $X^-\cdot H_2O$ complexes.[11]

In the context of intracluster proton transfer, the $OH^-\cdot H_2O$ complex (lower trace in Figure 2) is interesting because this symmetrical system represents a limiting situation where the proton-transfer shelf evolves into a small barrier in a double-minimum potential. In such a case, the quantum mechanical nature of the shared proton vibration is crucial. That is, the $OH^-\cdot H_2O$ complex has been demonstrated to actually adopt a symmetrical $[HO\cdots H\cdots OH]^-$ arrangement (i.e., with the excess charge equally distributed over both flanking OH groups), which must occur by averaging the electronic wave function over the spatially extended zero-point vibrational wave function of the shared proton.[15,27−34] Note that the symmetrical structure achieved after this zero-point averaging is taken into account yields an effective proton-transfer parameter, $\rho_{PT} = 0$. The $O^-\cdot H_2O$ curve is only slightly asymmetric relative to that of $OH^-\cdot H_2O$, yielding a scenario where its zero-point vibrational motion is anticipated to at least partially drive the ground state complex into the charge-delocalized regime.

To follow the extreme spectral shifts expected for the shared proton fundamentals in these complexes, this paper presents a survey of the vibrational bands in the 600−3800 cm^{-1} range using argon predissociation "messenger" infrared spectroscopy.[4,35] Some spectra have been reported earlier[4,15] for the Br^-, Cl^-, and F^- hydrates, but with the exception of $Cl^-\cdot H_2O$, these scans only covered the range of the OH stretching motions (>2600 cm^{-1}). Most importantly, this extension of spectral coverage to the low energy region of the infrared also enables us to evaluate the behavior of the HOH intramolecular bending fundamentals, as well as that associated with the frustrated rotations of the trapped water molecule. This additional information thus allows a much more complete characterization of the potential surfaces underlying the structure and dynamics of the anionic hydrogen bond.

II. Overview of $X^-\cdot H_2O$ Vibrational Spectroscopy

It is useful to first review the overall expectation for the six normal modes associated with the $X^-\cdot H_2O$ complexes. Two of these are derived from the high energy OH oscillators that are coupled in the isolated molecule to yield the symmetric and asymmetric stretching normal modes. The intramolecular bending fundamental (ν_b) lies at intermediate energy (1595 cm^{-1} in isolated H_2O),[23] and the three lowest energy modes correspond to the soft ion−molecule motions. Advanced theoretical methods (i.e., vibrational self-consistent field (VSCF)) have been applied to treat the anharmonic vibrational level structure of the F^- and Cl^- complexes,[12,36] with the results included in Table 2. The soft mode occurring highest in energy arises from the out-of-plane, frustrated rotation of the water molecule (ν_{oop}), while that occurring lowest in energy involves the ion−water stretching motion (ν_{iw}). Intermediate between these two lies the in-plane frustrated rotation (ν_{ip}) that leads to interconversion of the bound and free hydrogen atoms over the C_{2v} barrier in their double-minimum potential surfaces. The overall expectation from these calculations is that, as the strength of the anionic H-bond increases, the soft modes blue-shift while the shared proton stretch (ν_{IHB}) dramatically red-shifts. In fact, this red-shift becomes so large that the ν_{IHB} $v = 1$ level is predicted to tune *through* the $v = 1$ levels of both the ν_b and ν_{oop} modes, raising an interesting question of how these respective motions couple in the event of near-degeneracy.

In our earlier experimental studies[4,11,37] of the higher energy (>2600 cm^{-1}) bands in the $X^-\cdot H_2O$ (X = Cl, Br, and I) complexes, we were able to identify fundamental transitions of ν_{IHB} and ν_f, as well as bands associated with ν_b and ν_{iw} as

TABLE 2: Experimental and Theoretical Frequencies (cm^{-1}) for the $X^-\cdot H_2O$ [X = OH, O, F, Cl, and Br] Binary Complexes (the Experimental Error Is ± 5 cm^{-1} Unless Otherwise Noted)

	$OH^-\cdot H_2O$		$O^-\cdot H_2O$		$F^-\cdot H_2O$		$Cl^-\cdot H_2O$		$Br^-\cdot H_2O$	
vibrational mode[a]	expt	theory[b] (DMC)	expt	theory[c,d] (harmonic)	expt	theory[e] (CC-VSCF)	expt	theory[f] (CC-VSCF)	expt	theory[g] (anharmonic)
ν_{iw}		523		328		431	210[h]	194	158[h]	149
ν_{ip}	900−1140	1019/1106		534		581		265		264
ν_{oop}				1145	1083−1250	1166	745	694	664	654
$2\nu_{oop}$						2314	1402		1267	
ν_b				1527	1650	1645	1650	1633	1642	1618
$2\nu_b$						3265	3278		3264	
ν_{IHB}	697	655	767	1916	1523	1488	3130 (10)[i]	3151	3270	3227
$2\nu_{IHB}$					2905 (20)[i]	2888				
ν_f	3651/3670	3617/3636	3657	3853	3687	3640	3699	3735	3689	3685

[a] ν_{iw}, ion−water stretch; ν_{ip}, in-plane wag; ν_{oop}, out-of-plane wag; ν_b, HOH bend; ν_{IHB}, ionic hydrogen bond; ν_f, free OH stretch. [b] Reference 48. Values are an average of + and − fundamentals, which are split due to tunneling along the OH−OH torsional potential. [c] Unscaled frequencies. [d] Reference 51. [e] Reference 12. [f] Reference 36. [g] MP2/aug-cc-pVDZ anharmonic frequencies. [h] Observed as a combination band with the ionic hydrogen bond (IHB). [i] Large error (in parentheses) due to significant argon shift.

overtones and combinations. The infrared activity associated with shared proton excitation was particularly valuable, as it often appears with combination bands involving ν_{iw}, and exhibits band doubling traced to a strong Fermi-type mixing with the $v = 2$ level of ν_b.[4,37] These more complex patterns are obviously not recovered by the ubiquitous *ab initio* calculations of the harmonic cluster "spectra"[5,8,21,38,39] and are useful because they encode the dynamical response of the $X^-\cdot H_2O$ complexes to different types of vibrational excitation. Such anharmonic effects are particularly intriguing in the cases of primary interest here, where we expect the low frequency ν_{IHB} fundamentals to occur in the vibrationally mediated, intracluster proton-transfer regime.

III. Experimental Details

Argon-solvated cluster anions were generated by electron impact ionization (1 keV) of a pulsed free jet supersonic expansion and mass-selected in a tandem time-of-flight photofragmentation spectrometer described in detail previously.[40,41] For all of the species of interest (except the argon-tagged $OH^-\cdot H_2O$ cluster, which is included from previous work[32]), the $X^-\cdot H_2O\cdot Ar$ complexes were synthesized using an entrainment approach,[42] where trace amounts of the neutral precursor (CH_2Br_2, $CHCl_3$, NF_3, and N_2O for the Br^-, Cl^-, F^-, and O^- anions, respectively) and H_2O vapor were introduced just outside the nozzle with independently controlled pulsed valves.

Infrared spectra were recorded via argon predissociation spectroscopy:[4,35]

$$X^-\cdot H_2O\cdot Ar_n + h\nu \rightarrow X^-\cdot H_2O\cdot Ar_m + (n-m)\,Ar \quad (3)$$

where the argon-solvated anionic clusters were photoexcited with infrared pulses (600−1900 and 2200−3800 cm^{-1}, ~3 cm^{-1} resolution) generated by a 10 Hz Nd:YAG pumped, KTP/KTA/$AgGaSe_2$-based OPO/OPA laser (Laser Vision). The spectra result from the addition of 30−40 individual scans and were normalized for variations in laser pulse energy over the respective spectral ranges. The spectra of the two regions are reported with normalization to the largest peak in each range because the significant difference in output beam shape from the different mixing schemes makes it difficult to determine quantitative relative photofragmentation cross sections. The entire path of the infrared laser beam up to the vacuum chamber was thoroughly purged with dry air to ensure minimal variation of laser power due to absorption of ambient water vapor in both spectral regions.

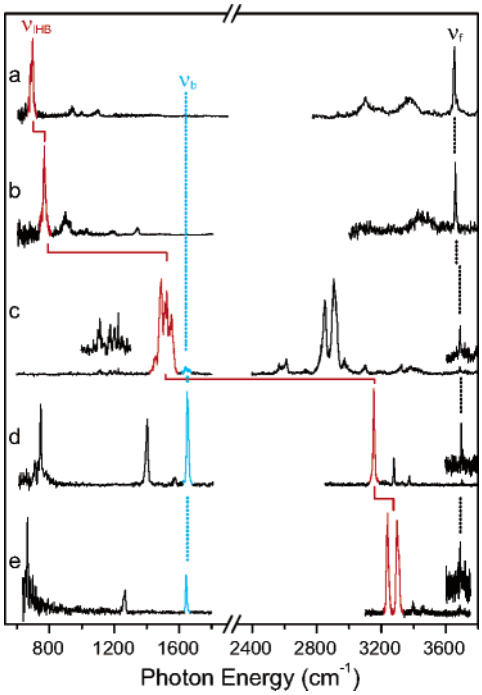

Figure 3. Argon predissociation infrared spectra of the (a) $OH^-\cdot H_2O\cdot Ar$, (b) $O^-\cdot H_2O\cdot Ar$, (c) $F^-\cdot H_2O\cdot Ar$, (d) $Cl^-\cdot H_2O\cdot Ar_m$, and (e) $Br^-\cdot H_2O\cdot Ar_n$ complexes, with the anion proton affinity decreasing down the figure. For Cl^-, $m = 1$ in the lower region and $m = 11$ in the upper region, whereas, for Br^-, $n = 1$ in the lower region and $n = 3$ in the upper region. The bands associated with the fundamental transition of the ionic hydrogen bond (denoted ν_{IHB}) are highlighted in red, while the evolution of the HOH bend mode (ν_b) is highlighted in blue. The nonbonded OH stretch (ν_f) is indicated by a black dotted line.

IV. Results and Discussion

IVA. Survey of the $X^-\cdot H_2O$ Argon Predissociation Vibrational Spectra. The vibrational predissociation spectra of the $X^-\cdot H_2O$ complexes (X = O, F, Cl, and Br) are presented in Figure 3b−e along with that of the previously reported[31,34] $OH^-\cdot H_2O$ cluster in the top trace (3a) for comparison. The spectra are arranged so that the X^- proton affinity increases from bottom to top. All of these SIHB complexes display sharp, but weak free OH stretch (ν_f) features near the ~3707 cm^{-1} centroid of the OH stretches in the isolated water molecule.[23] As expected, the hydrogen atoms engaged in the ionic H-bond contribute much stronger IR fundamentals that occur dramatically red-shifted from ν_f in a manner that is highly dependent upon the identity of the anion.[11] These ν_{IHB} bands are considered

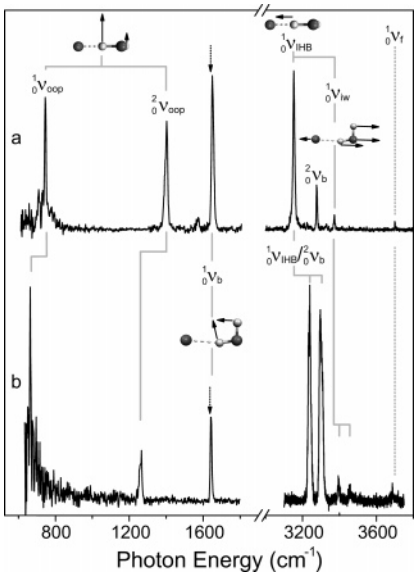

Figure 4. Expanded view of the (a) $Cl^-\cdot H_2O$ and (b) $Br^-\cdot H_2O$ spectra, highlighting assignments of the ν_b, ν_{oop}, and ν_{IHB} transitions. Also apparent in the higher energy region of both spectra are the combination bands involving ν_{IHB} and the ion−molecule stretching soft mode (ν_{iw}). Dotted arrows indicate the expected position of ν_b based upon the unperturbed band positions of the overtone (e.g. $^1/_2(2\nu_b)$). The notation $^i\nu$ indicates the number of quanta (i) in the upper level of the transition.

in detail below and are highlighted in red. The sharp band arising from the HOH intramolecular bending fundamental (ν_b) near 1600 cm^{-1} (highlighted in blue in Figure 3) is clear in the Br^- and Cl^- complexes but appears more diffuse in $F^-\cdot H_2O$ and finally completely disappears in the $O^-\cdot H_2O$ and $OH^-\cdot H_2O$ spectra. The most important qualitative feature in this series is the extreme variation of the shared proton transitions such that, as the basicity of the anion increases, the fundamental ν_{IHB} band first drops below ν_b in $F^-\cdot H_2O$ before stabilizing in the $O^-\cdot H_2O$ and $OH^-\cdot H_2O$ spectra near the expected location of the out-of-plane frustrated rotation in the $Cl^-\cdot H_2O$ complex (see Table 2).[15] This represents a red shift of over 3000 cm^{-1} for the OH stretching motion in strong anion−water complexes compared to that of free H_2O.

IVB. $Cl^-\cdot H_2O$ and $Br^-\cdot H_2O$: Charge-Localized Complexes. Because the heavier halide ions (X = Cl^- and Br^-) have rather low proton affinities,[23] both the ν_f and ν_{IHB} fundamentals appear in the higher energy (2400−3800 cm^{-1}) range and have been analyzed in an earlier report.[4] The fact that the ν_{IHB} fundamentals occur relatively close to ν_f is consistent with expectations from the potentials in Figure 2, where the shelf lies very high in energy (14 000 cm^{-1} in $Cl^-\cdot H_2O$) so that the system can be regarded as a largely intact water molecule interacting with the mostly charge-localized anion in both the ground and vibrationally excited states. Figure 4 highlights the spectra of these two complexes to facilitate the discussion of the band assignments. Note that the low energy (<1800 cm^{-1}) $Br^-\cdot H_2O$ pattern is reported here for the first time. The $Cl^-\cdot H_2O$ spectrum was reported earlier[15] in the region above 1000 cm^{-1}, which therefore missed the strong transition at 745 cm^{-1}.

We previously exploited[4,11] the systematic variation of the (3000−3800 cm^{-1}) bands through the X^- = Cl^-, Br^-, and I^- series to assign the ν_{IHB} fundamentals and combination bands involving ν_{IHB} excitation with concomitant excitation of the lowest frequency soft mode corresponding to the ion−water stretch (ν_{iw} in Figure 4). This analysis revealed that the ion-bound OH stretch tunes into accidental degeneracy with the 2 ← 0 overtone of the intramolecular bending vibration (ν_b) in the $Br^-\cdot H_2O$ complex, giving rise to band doubling from the resulting Fermi-resonance interaction.[4,37]

To aid in the assignments of the lower energy peaks, the locations of the ν_b bending fundamentals could be estimated at the harmonic level as $^1/_2(2\nu_b)$, where the unperturbed energies of the overtone ($2\nu_b$) levels were extracted from a simple 2 × 2 deperturbation analysis of the Fermi doublets. These harmonic estimates are indicated by dotted arrows in the $Cl^-\cdot H_2O$ and $Br^-\cdot H_2O$ spectra in Figure 4a and b, which fall quite close to the observed sharp transitions near 1650 cm^{-1} in both cases. This agreement both validates the assignments of the bend overtone as the partner in the Fermi diad near 3200 cm^{-1} and enables us to determine that the anharmonicity of the intramolecular bending vibration is quite small ($\omega_e\chi_e$ = 8.5 and 10 cm^{-1} for Cl^- and Br^-, respectively), as indicated in Table 2.

The discussion above indicates that the HOH bend and OH stretching bands of the $Cl^-\cdot H_2O$ and $Br^-\cdot H_2O$ complexes are readily understood in the context of fundamentals, combination bands, and Fermi resonances. To complete our experimental survey of the complex vibrations, we now turn to the direct interrogation of the soft modes. Although calculations (Table 2) indicate that we only expect to observe the out-of-plane vibration (ν_{oop}) in our frequency window (>600 cm^{-1}), two bands are observed for the $Cl^-\cdot H_2O$ and $Br^-\cdot H_2O$ complexes, with the higher energy transition appearing much too high for a fundamental. The lowest energy bands at 745 and 664 cm^{-1} appear close to the calculated values for ν_{oop} (694 and 654 cm^{-1}, respectively for Cl^- and Br^-), and we assign them to these fundamentals, as indicated in Figure 4. The calculated normal mode displacement vectors are included in the insets, indicating that this motion could be equivalently regarded as a vibration of the shared proton perpendicular to the H-bond axis. Note that this vibration is calculated to lie much higher in energy than both the in-plane vibration at ∼250 cm^{-1} and the ion−molecule stretch at ∼175 cm^{-1}.

Having assigned the lowest observed transitions in $Cl^-\cdot H_2O$ and $Br^-\cdot H_2O$ to the ν_{oop} fundamentals, we next consider the origin of the interlopers in both spectra in the 1200−1400 cm^{-1} range. In each case, the extra band occurs near the expected location of $2\nu_{oop}$ (Table 2), and in fact, the 1402 cm^{-1} feature in $Cl^-\cdot H_2O$ has been previously assigned to the 2 ← 0 overtone of the out-of-plane mode in our analysis[15] of the $Cl^-\cdot H_2O$ spectrum in the 1000−1900 cm^{-1} region. The fact that these levels are reasonably harmonic is particularly interesting because the overtones appear with almost the same intensities as the fundamentals! As such, the mechanism for this unusually strong overtone excitation is not likely to involve mechanical anharmonicity alone. Intensity borrowing via Fermi resonance with the bend fundamental can also be ruled out, as both the bend fundamental and the out-of-plane overtone transitions occur where expected for a harmonic model where the level positions are extrapolated from the ν_{oop} and $2\nu_b$ energy levels. We will consider the origin of the anomalous ν_{oop} overtone intensity in section IVF.

With this direct observation of ν_{oop} and the indirect detection of ν_{iw} as a combination band with the ν_{IHB} fundamental, five of the six $X^-\cdot H_2O$ modes are now revealed experimentally. The only mode that is left to be established experimentally is therefore the in-plane vibrational motion (ν_{ip}) that interconverts the asymmetric SIHB complexes through the C_{2v} transition state. It is interesting that this motion is not significantly activated upon excitation of the shared proton in the monatomic $X^-\cdot H_2O$ complexes but was found to play a dominant role in the spectra

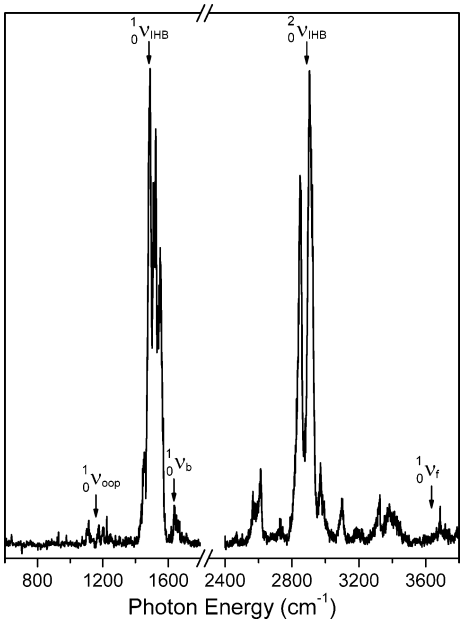

Figure 5. Expanded view of the $F^-\cdot H_2O$ spectra, with assignments based upon the work by Xantheas and co-workers.[12] The arrows denote the predicted locations of transitions arising from the ionic H-bonded OH stretch (ν_{IHB}), nonbonded OH stretch (ν_f), HOH intramolecular bend (ν_b), and out-of-plane frustrated rotation of the water molecule (ν_{oop}), obtained using the CC-VSCF treatment of the anharmonic vibrations. The notation $^i\nu$ indicates the number of quanta (i) in the upper level of the transition. Note the number of weaker bands appearing throughout the higher energy region.

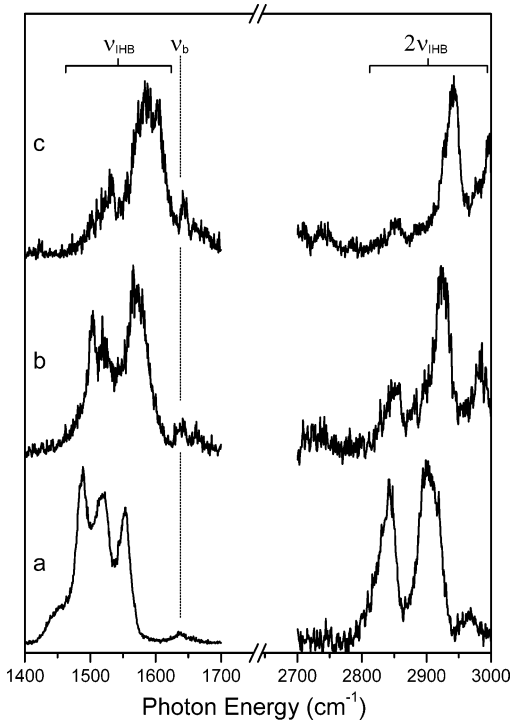

Figure 6. Argon cluster size dependence of the $F^-\cdot H_2O\cdot Ar_n$ spectra in the ν_{IHB} fundamental and overtone regions, for (a) $n = 1$, (b) $n = 2$, and (c) $n = 3$.

of water complexes involving a triatomic binding site (e.g., $-CO_2^-$) on the anion.[43,44]

IVC. $F^-\cdot H_2O$: Vibrationally Induced Intracluster Proton Transfer. With the behavior of the more charge-localized complexes in mind, we now turn to the $F^-\cdot H_2O$ complex, with the entire spectrum highlighted in Figure 5 and an expanded view of the free OH region presented in Figure 7d. Although the low energy region of the $F^-\cdot H_2O$ spectrum appears dramatically different than those of $Cl^-\cdot H_2O$ and $Br^-\cdot H_2O$, this difference largely reflects the shift of the ν_{IHB} band below that of the water bend and the expected increase in its intensity compared to the vibrations at play in $Cl^-\cdot H_2O$ and $Br^-\cdot H_2O$. In fact, the relative intensities of the ν_{IHB}, ν_{oop}, and ν_b bands are in agreement with those obtained from harmonic calculations. In this case, the $2\nu_{oop}$ band, calculated[12] to occur at 2314 cm^{-1} in the $F^-\cdot H_2O$ spectrum, would not have been recovered in the scan range, as the available laser power becomes quite low at the lower energy limit of the KTA-based mixing stage, leading us to only report the action spectra down to 2400 cm^{-1}.

Schaefer and co-workers[26] were the first to consider the shared proton vibrations in $F^-\cdot H_2O$ and pointed out that, while the complex indeed corresponds to a largely charge-localized $F^-\cdot H_2O$ arrangement at the zero-point vibrational level of the shared proton, the first vibrationally excited level would occur *over* the shelf in the potential, dramatically lowering the ν_{IHB} fundamental transition to around 1667 cm^{-1}. On the basis of this expectation, we therefore previously assigned the observed[45] multiplet centered at 2930 cm^{-1} to $2\nu_{IHB}$. This transition occurs remarkably close to Schaefer's prediction[26] (2967 cm^{-1}) based on a numerical solution to the vibrational Schrödinger equation for the one-dimensional potential (Figure 2). Subsequent theoretical work along these lines using a more accurate potential surface by Kim and co-workers[8] supported this general assignment scheme. The refined one-dimensional treatment[8] places

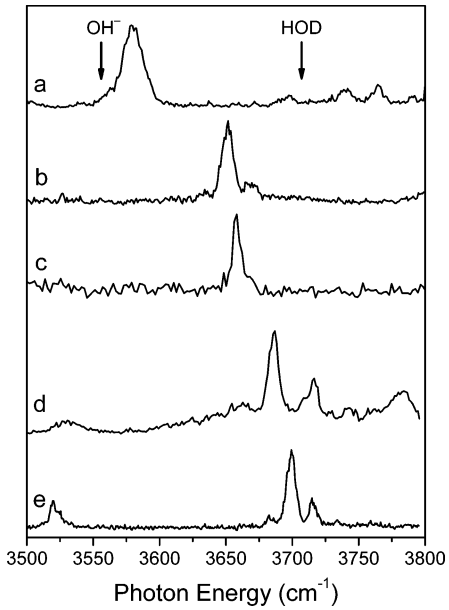

Figure 7. Expanded view of the nonbonded OH stretching transition in the $X^-\cdot H_2O$ spectra. Trace (a) corresponds to the charge-localized hydroxide complex, $OH^-\cdot N_2O$.[50] The left arrow labeled OH^- indicates the band origin of the isolated hydroxide anion (3556 cm^{-1}), while the arrow on the right (HOD) indicates the OH stretch transition in isolated HOD.[23] Traces (b)−(e) correspond to the $X^-\cdot H_2O\cdot Ar_n$ clusters for (b) X = OH, $n = 1$, (c) X = O, $n = 2$, (d) X = F, $n = 1$, and (e) X = Cl, $n = 1$.

the ν_{IHB} fundamental at 1481 cm^{-1}, close to the strong triplet in the observed spectrum centered at 1523 cm^{-1}.

Of course, one can question the validity of a one-dimensional treatment for such a large amplitude motion of the shared proton, and Chaban and co-workers[12] recently reported a full-dimensional, correlation-corrected vibrational self-consistent field (CC-

VSCF) treatment on a CCSD(T)/aug-cc-pVTZ potential surface, with the results included in Table 2 and indicated by arrows in Figure 5. The agreement for most of the transitions is outstanding, with the largest error interestingly occurring for the free OH stretch, which is predicted to occur about 50 cm^{-1} below the observed band. On the basis of this overall agreement, we offer the assignments indicated in Figure 5 and Table 2.

In the previous observation[45] of the higher energy $2\nu_{IHB}$ transition, we noted that this feature appears as a distinct multiplet that was strongly argon-dependent, unlike the persistent, Fermi-split doublet found in the $Br^-\cdot H_2O$ spectrum. We therefore surveyed the argon dependence of the $F^-\cdot H_2O$ 1500 cm^{-1} band with the results displayed in Figure 6. The general trend is that the bands blue-shift upon the addition of argon atoms, with the multiplet structure evolving in a complicated fashion. Note that the fundamental bands exhibit similar behavior to that reported for the putative overtone, lending empirical support to the assignment scheme. Indeed, the spacing between the multiplets in the $2\nu_{IHB}$ state ($\sim$64 cm^{-1}) is twice that obtained here for the fundamental ($\sim$32 cm^{-1}), confirming that these splittings share the same origin.

The large argon-induced blue shift of the ν_{IHB} transitions is readily understood as a consequence of the fact that excitation of this vibration causes charge delocalization in the vibrationally excited state. Specifically, the different electronic character of the ground vibrational state relative to that of the excited levels leads to a differential solvation effect, where the more charge-localized ground state is better solvated than the more delocalized excited states, pushing the levels apart as more argon atoms surround the F^- ion at the zero-point level of the complex. When we have such large argon shifts, there are generally multiple nearby bands arising from the isomer distribution of argon attachment sites,[46] and it is difficult to be definitive about which transitions result from isomers and which from possible band mixing. It would therefore be useful to capture a spectrum of this species in isolation (i.e., without a messenger) to clarify the fine structure assignments. The latter possibility arises because combination bands between the out-of-plane wag and the ion−molecule stretch, among others, are close to ν_{IHB} and could conceivably mix through higher order terms in the potential.

IVD. Comparison of $OH^-\cdot H_2O$ and $O^-\cdot H_2O$: Charge-Delocalized Ground-State Species. The two upper traces in Figure 3 compare the $O^-\cdot H_2O$ spectrum with that of $OH^-\cdot H_2O$, and the most important observation is that the spectra are remarkably similar; both are dominated by sharp and relatively strong free OH stretch transitions and display an isolated ν_{IHB} band at very low energy. In fact, the 767 cm^{-1} band in $O^-\cdot H_2O$ lies only 70 cm^{-1} above the 697 cm^{-1} shared proton fundamental in the symmetrical $OH^-\cdot H_2O$ complex, strongly suggesting a similar assignment in the asymmetric system. As mentioned in the Introduction, the $OH^-\cdot H_2O$ system has been shown to correspond to a situation where the zero-point motion of the shared proton lies above a barrier in a double-minimum potential surface, as shown in Figure 2. The fact that the ν_{IHB} energies in $O^-\cdot H_2O$ and $OH^-\cdot H_2O$ are so similar implies that the zero-point level of the former also lies very near or even above the proton-transfer barrier. Indeed, a one-dimensional numerical solution to the (MP2/aug-cc-pVDZ level of theory) potential shown in Figure 2 places the $v = 0$ level $\sim$70 cm^{-1} above the barrier. On the other hand, Chipman and Bentley[47] have recently considered this potential surface at length and find the shapes to be strongly dependent on the level of theory. Consequently, further work will be required to pin down the exact location of the barrier relative to the zero-point vibrational level in this system.

Further support for the conclusion that $O^-\cdot H_2O$ occurs with the shared proton zero-point level close to the barrier can be derived from the behavior of the free OH stretching bands. In particular, because the excess charge is delocalized over both nonbonded OH groups in $OH^-\cdot H_2O$, its ν_f band occurs significantly to the red of the position in the charge-localized $X^-\cdot H_2O$ complexes, as the OH moiety adopts the character of the hydroxide ion, which has a vibrational frequency about 150 cm^{-1} below that of an OH stretch in isolated water. Figure 7 presents an expanded view of the critical free OH stretching bands of $X^-\cdot H_2O$ (X = OH, O, F, and Cl), in addition to that of the $OH^-\cdot N_2O$ complex, where the excess charge is almost entirely located on the OH moiety. The two arrows indicate the locations of the vibrational band origins of isolated OH^- (left) and HOD (right) for reference.[23] Casual inspection of Figure 7 reveals that there is a strong correlation between the frequency of the free OH stretch in a complex and the extent to which the excess charge is distributed over these atoms. Thus, the close proximity of the red-shifted ν_f stretches in $O^-\cdot H_2O$ and $OH^-\cdot H_2O$, combined with the similarity of their low energy transitions arising from the shared proton, establish that both of these complexes exhibit extensive charge delocalization in their vibrational ground states.

Our main emphasis in this paper is to expose the general trends in the spectra over all of the complexes, and in this sense, the OH^- and O^- spectra are quite simple in that they each have only two dominant bands, one from the parallel shared proton stretch and the other from the free OH. In this context, we remark that the strong frustrated rotations, evident in the Cl^- and Br^- complexes, become harder to distinguish from the intramolecular water bend in the more strongly interacting systems. Specifically, in the $OH^-\cdot H_2O$ system, once zero-point motion is considered, the most probable structure has the central hydrogen atom equidistant from the two oxygen atoms.[48] Consequently, motions that had been described as water bends become the symmetry adapted combinations of displacements of the outer hydrogen atoms, termed wags and rocks, which have a minor contribution from displacements of the central hydrogen atom. At the same time, the perpendicular displacements of the central hydrogen atom have significant intramolecular water bend character. In collaboration with Bowman and co-workers, we recently performed a detailed analysis of the $OH^-\cdot H_2O$ spectrum.[48] We found that vibrational CI calculations predict that the fundamentals associated with perpendicular displacements of the central hydrogen atom occur in the 1300−1500 cm^{-1} range, which are indeed much higher than the analogous modes in Cl^- and Br^-, but there is very little activity in the $OH^-\cdot H_2O$ spectrum in this region. Fixed node diffusion Monte Carlo calculations predict that the states that have nodes along these coordinates will have frequencies near the observed bands at 1000 cm^{-1}. Preliminary analysis of these states, using the potential and dipole moment surfaces developed by Huang et al.,[33,48] indicates that they are best described as combination bands or overtones involving the OO stretch, ν_{IHB}, as well as the outer OH wag and rock, and that the relative intensities of these bands are consistent with the observed intensities in the $OH^-\cdot H_2O$ spectrum in the 1000 cm^{-1} region.

The $O^-\cdot H_2O$ complex displays several transitions in the 900−1800 cm^{-1} region, but the assignment of these features will undoubtedly require fully anharmonic calculations on a realistic potential surface. The latter is, of course, more difficult due to the fact that this is an open shell system. In closing this

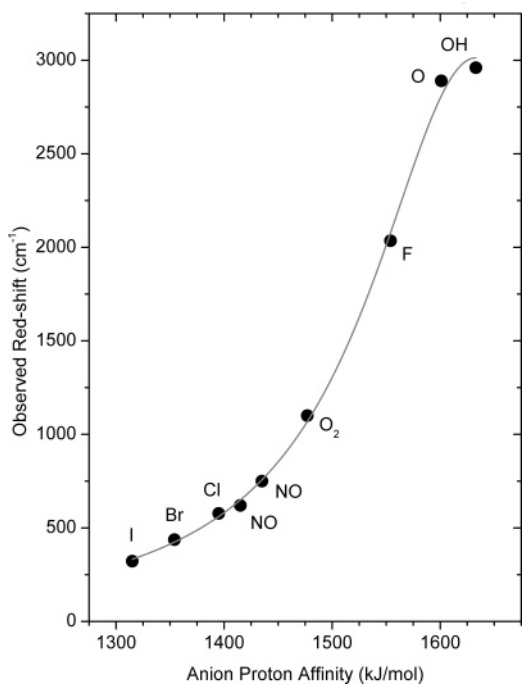

Figure 8. Observed red-shift (cm^{-1}) for the shared proton vibration as a function of the anion proton affinity for the $X^-\cdot H_2O$ binary complexes. For NO^-, the lower energy value corresponds to the O-bound isomer, whereas the higher energy point is for the N-bound isomer, where both values are corrected for the electron-spin-conserving intracluster proton-transfer asymptote.[11]

discussion of the minor features, we note that two very broad bands in the $OH^-\cdot H_2O$ spectrum around 3000−3200 cm^{-1} were initially assigned as overtones of the shared proton stretch, but this identification was subsequently rejected on the basis of the observed, very low energy fundamental.[31,34] Interestingly, $O^-\cdot H_2O$ displays a similarly broad band at 3350 cm^{-1}, and it would be valuable to unravel the molecular physics underlying these broad structures.

IVE. Correlation between the Shared Proton Stretch and the Anion Basicity: Summary of Overall Trends. We have noted previously that the magnitudes of the ν_{IHB} red shifts in many atomic and molecular anion monohydrates are strongly correlated with the proton affinity (PA) of the anion.[11] The earlier work was limited to shifts of less than 1000 cm^{-1}, however, and the present data set allows us to explore this trend over a much larger range. Figure 8 presents the PA dependence of the observed shifts for the complexes studied here, together with the values for several other previously reported systems. The correlation with PA is indeed maintained over a sufficiently large range of shifts that the overall sigmoidal shape of this dependence is now revealed. Interestingly, there is an inflection point in the neighborhood of the $F^-\cdot H_2O$ value, a complex where the intracluster proton-transfer shelf is calculated to occur just below the $v = 1$ level of the shared proton vibration. It is now clear that the very strongly red-shifted stretch in the $OH^-\cdot H_2O$ complex occurs because the shelf falls below the zero point, yielding an asymptotic value for the shift expected for a proton engaged in a three-center, two-electron covalent bond. For example, the prototypical $BrHBr^-$ and $ClHCl^-$ species exhibit shared proton stretches at 733 and 723 cm^{-1}, respectively,[18,19] close to the observed values in the O^- (767 cm^{-1}) and OH^- (697 cm^{-1}) complexes.

As the proton becomes more equally shared in the O^- and OH^- hydrates, the intramolecular bending vibration associated with an intact water molecule is lost. The free OH transition also provides an independent signature of the emergent covalent behavior because of the concomitant delocalization of the excess charge over both oxygen atoms. Specifically, the ν_f bands in the more charge-localized systems (Cl^-, Br^-) occur near the OH stretch position in isolated HOD (3707 cm^{-1}), but as delocalization becomes important, ν_f red-shifts toward the fundamental vibration of the bare hydroxide ion (3556 cm^{-1}). Thus, the complexes for which the zero-point motion of the shared proton occurs over the barrier exhibit the largest ν_f red shift, while the fluoride hydrate, with a zero-point level falling below the shelf, displays a more typical nonbonded OH stretch as well as an intact intramolecular bending transition. The intracluster proton-transfer process is driven by selective excitation of the ν_{IHB} vibrations of the fluoride complex, however, and its spectrum is indeed most cluttered with significant structure scattered throughout the entire spectral region. A fertile direction for future work is therefore to extend the fully anharmonic calculations on the $F^-\cdot H_2O$ potential surface to identify the motions responsible for these extra bands.

IVF. Remarks on the Origin of the Unusual Overtone Intensities of the Out-of-Plane Bend in $F^-\cdot H_2O$, $Cl^-\cdot H_2O$, and $Br^-\cdot H_2O$. Most aspects of the $X^-\cdot H_2O$ spectral behavior can be intuitively understood as a consequence of intracluster charge delocalization. In particular, the anharmonic nature of the shared proton vibrations is readily explained by strong deformations in the potential for basically one-dimensional motion. One curious aspect of the spectra, however, is the observation of very intense overtones of the out-of-plane (oop) bending transitions in the $Br^-\cdot H_2O$ and $Cl^-\cdot H_2O$ complexes (Figure 4), especially in light of the fact that, on the basis of the energies of the levels involved, they appear to be largely harmonic, and there is no evidence for strong Fermi interactions. In the limit where the electronic structure is frozen at the equilibrium geometry, oop displacement gives rise to a perpendicular component in the dipole moment (μ_{perp}):

$$\mu_{perp}(Q_{oop}) \sim \left.\frac{d\mu_{perp}}{dQ}\right|_{eq} Q_{oop} \qquad (4)$$

and the usual $\Delta v = +1$ selection rule, with a perpendicular orientation of the transition moment. In this limit, the overtone is strictly forbidden by symmetry.

To explore the origin of the anomalous overtone intensity, we calculated (MP2/aug-cc-pVTZ level of theory/basis using Gaussian 03)[22] the electronic structure changes for displacements along the oop coordinate (Q_{oop}), defined as the angle between the bonding OH bond axis and the plane that contains the free OH bond and the halide ion. A useful way to gauge qualitative features of the dipole surface associated with these distortions is to follow the evolution of the Mulliken charges (extracted from these calculations) on the atoms, which are displayed in Figure 9 for the $Cl^-\cdot H_2O$ complex. Similar behavior is observed for the other complexes. Note that the classical turning points of the oop wave function at the zero-point level occur at about 20° where the major deformation is perpendicular displacement of the shared proton (relative to the H-bond axis), as illustrated in the upper left inset of Figure 4. Inspection of Figure 9 reveals that excursions along Q_{oop} result in considerable (20%) charge redistribution from the water molecule back onto the Cl atom. This electronic structure change thus gives rise to a modulation of the dipole moment *parallel* to the H-bond axis [$\mu_{par}(Q_{oop})$] in a manner that is *symmetrical* in the Q_{oop} displacements! As

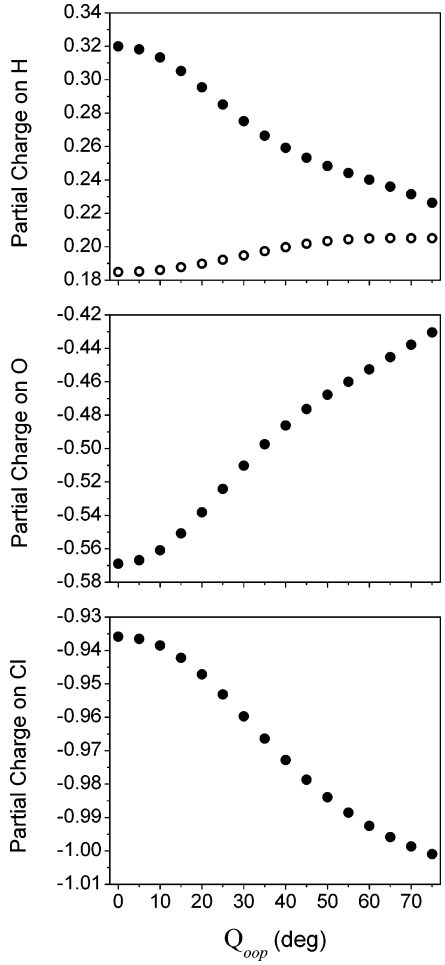

Figure 9. Mullikin charges of the four atoms in $Cl^-\cdot H_2O$ are plotted as a function of Q_{oop}, the angle between the OH bond axis of the shared proton and the plane that contains the free OH bond and the halide ion. In the case of the hydrogen atoms, the hydrogen that participates in the hydrogen bond is shown with filled circles[12] and the free hydrogen is shown in open circles.

a result, Taylor expansion of the parallel modulation of the dipole moment has a leading quadratic term:

$$\mu_{par}(Q_{oop}) \sim \left.\frac{d^2\mu}{dQ^2}\right|_{eq} Q_{oop}^2 + ... \qquad (5)$$

and thus would contribute a $\Delta v = 2$ selection rule for a transition dipole oriented along the bond axis. Moreover, the calculated dipole surface cuts indicate that this effect is large. For example, in the $Cl^-\cdot H_2O$ case, evaluation of the dipole derivatives at the equilibrium geometries predicts the overtone to be on the same order as the fundamental (in the harmonic limit) with a ratio of $I(0-2/0-1) = 0.70$, in good agreement with the ratio seen in the experimental spectrum (Figure 4).

The qualitative picture resulting from this analysis is intuitive and general: Rotation of the hydrogen away from the bond axis acts to partially break the H-bond, resulting in charge redistribution from the water molecule back to the halide ion. Calculations indicate that the effect is significant in all of the halide monohydrates. Of course, the actual wave functions at play exhibit large amplitude displacements in the first few energy levels, and therefore, even in a one-dimensional treatment, the explicit Q_{oop} dependence of all three vector components of μ as well as the anharmonicities of the wave functions must be taken into account. More accurate calculations including these aspects have been performed and result in a small reduction of the predicted overtone intensity ($I(1 - D)/I(\text{harmonic}) = 0.83$), but the qualitative effect survives. Interestingly, this reduction in intensity results from contributions of higher order terms in the expansion of the dipole moment and not anharmonicities in the potential. This provides further evidence for the picture that the intensity of the υ_{oop} overtone mostly reflects charge redistribution when the H-bond is broken. Similar effects are found in the fluoride and bromide complexes.

What remains is to extend this treatment using much more sophisticated, full-dimensional vibrational eigenfunctions and the entire dipole surface, but the simple one-dimensional model, presented in the spirit of highlighting general trends in the $X^-\cdot H_2O$ systems, appears to capture the basic physics encoded in the unusual intensities displayed by the oop mode. Encouragingly, Rheinecker and Bowman find that full-dimensional calculations of the vibrational spectrum of $Cl^-\cdot H_2O$ using *ab initio* potential and dipole moment surfaces indeed exhibit a large intensity in the first overtone of υ_{oop}.[49]

V. Summary

Argon predissociation spectra of the $X^-\cdot H_2O$ (X = OH, O, F, Cl, and Br) complexes are reported in the 600−1900 and 2400−3800 cm^{-1} regions. The dominant band arising from the shared proton stretch is observed to systematically red-shift by over 3000 cm^{-1} relative to the position in a bare water molecule in a manner that is strongly correlated with the proton affinity of the anion. In the very strongly basic O^- and OH^- complexes, the loss of the independent fabric of the water molecule is immediately evident by the disappearance of the HOH intramolecular bending vibration. Closer inspection of the nonbonded OH stretching transitions reveals that these bands also red-shift toward the location of the hydroxide ion as intramolecular proton transfer drives charge delocalization over both oxygen atoms. Thus, while the $O^-\cdot H_2O$ and $OH^-\cdot H_2O$ clusters are calculated to be more charge-localized complexes at their minimum energy geometries, large amplitude displacements of the shared proton in the vibrational zero-point levels account for the experimentally observed charge-delocalized ground state structures. The spectra displayed by most of the complexes are quite simple, but that of $F^-\cdot H_2O$ appears more complex with many significant features scattered throughout the spectrum. We trace this increased activity to an intermediate regime where vibrational excitation of the shared proton drives the system from a charge-localized ground state to a charge-delocalized configuration in the excited state. With this new spectroscopic information, five of the six expected $X^-\cdot H_2O$ normal modes are now characterized experimentally, so that the only mode yet to be revealed is the in-plane frustrated rotation motion that interconverts the two hydrogen atoms from the free OH to the H-bonded site in these asymmetric, single H-bonded complexes.

Note Added in Proof. While this paper was in preparation, preliminary infrared spectra extending to 1975 cm^{-1} were obtained for the $Cl^-\cdot H_2O$ species. This data reveals a transition at 1960 cm^{-1} which is tentatively assigned to the combination band of ν_b and ν_{ip}, implying a value for ν_{ip} of ~310 cm^{-1}. This assignment is supported by *ab initio* (MP2/aug-cc-pVTZ) anharmonic calculations[22] which place this combination band at 1952 cm^{-1} and predict $\nu_{ip} = 334$ cm^{-1}. Further studies are currently being performed, which will shed light on the location of this transition in other halide monohydrates and determine the effect of tunneling across the barrier which interconverts the two hydrogens.

Acknowledgment. M.A.J. and A.B.M. thank the Physical Chemistry Division of the National Science Foundation for generous support of this work. We also thank Jaime L. Rheinecker and Professor Joel M. Bowman for sharing the results of their calculations on the $Cl^-\cdot H_2O$ system prior to publication.

References and Notes

(1) Johnson, M. S.; Kuwata, K. T.; Wong, C.-K.; Okumura, M. *Chem. Phys. Lett.* **1996**, *260*, 551.
(2) Xantheas, S. S. *J. Phys. Chem.* **1996**, *100*, 9703.
(3) Choi, J.-H.; Kuwata, K. T.; Cao, Y.-B.; Okumura, M. *J. Phys. Chem. A* **1998**, *102*, 503.
(4) Ayotte, P.; Weddle, G. H.; Kim, J.; Johnson, M. A. *J. Am. Chem. Soc.* **1998**, *120*, 12361.
(5) Cabarcos, O. M.; Weinheimer, C. J.; Lisy, J. M.; Xantheas, S. S. *J. Chem. Phys.* **1999**, *110*, 5.
(6) Irle, S.; Bowman, J. M. *J. Chem. Phys.* **2000**, *113*, 8401.
(7) Thompson, W. H.; Hynes, J. T. *J. Am. Chem. Soc.* **2000**, *122*, 6278.
(8) Kim, J.; Lee, H. M.; Suh, S. B.; Majumdar, D.; Kim, K. S. *J. Chem. Phys.* **2000**, *113*, 5259.
(9) Bieske, E. J.; Dopfer, O. *Chem. Rev.* **2000**, *100*, 3963.
(10) Vanden, T. D.; Forinash, B.; Lisy, J. M. *J. Chem. Phys.* **2002**, *117*, 4628.
(11) Robertson, W. H.; Johnson, M. A. *Annu. Rev. Phys. Chem.* **2003**, *54*, 173.
(12) Chaban, G. M.; Xantheas, S. S.; Gerber, R. B. *J. Phys. Chem. A* **2003**, *107*, 4952.
(13) Duncan, M. A. *Int. Rev. Phys. Chem.* **2003**, *22*, 407.
(14) Bowman, J. M.; Xantheas, S. S. *Pure Appl. Chem.* **2004**, *76*, 29.
(15) Diken, E. G.; Headrick, J. M.; Roscioli, J. R.; Bopp, J. C.; Johnson, M. A.; McCoy, A. B.; Huang, X.; Carter, S.; Bowman, J. M. *J. Phys. Chem. A* **2005**, *109*, 571.
(16) Meot-Ner, M. *Chem. Rev.* **2005**, *105*, 213.
(17) Gerhards, M.; Unterberg, C.; Gerlach, A. *Phys. Chem. Chem. Phys.* **2002**, *4*, 5563.
(18) Pivonka, N. L.; Kaposta, C.; Brummer, M.; Helden, G. v.; Meijer, G.; Woste, L.; Neumark, D. M.; Asmis, K. R. *J. Chem. Phys.* **2003**, *118*, 5275.
(19) Kawaguchi, K. *J. Chem. Phys.* **1988**, *88*, 4186.
(20) Okumura, M.; Choi, J.-H.; Kuwata, K. T.; Cao, Y.-B.; Haas, B.-M. *Proc. SPIE* **1995**, *2548*, 147.
(21) Baik, J.; Kim, J.; Majumdar, D.; Kim, K. S. *J. Chem. Phys.* **1999**, *110*, 9116.
(22) Frisch, M. J.; Trucks, G. W.; Schlegel, H. B.; Scuseria, G. E.; Robb, M. A.; Cheeseman, J. R.; Montgomery, J. A., Jr.; Vreven, T.; Kudin, K. N.; Burant, J. C.; Millam, J. M.; Iyengar, S. S.; Tomasi, J.; Barone, V.; Mennucci, B.; Cossi, M.; Scalmani, G.; Rega, N.; Petersson, G. A.; Nakatsuji, H.; Hada, M.; Ehara, M.; Toyota, K.; Fukuda, R.; Hasegawa, J.; Ishida, M.; Nakajima, T.; Honda, Y.; Kitao, O.; Nakai, H.; Klene, M.; Li, X.; Knox, J. E.; Hratchian, H. P.; Cross, J. B.; Adamo, C.; Jaramillo, J.; Gomperts, R.; Stratmann, R. E.; Yazyev, O.; Austin, A. J.; Cammi, R.; Pomelli, C.; Ochterski, J. W.; Ayala, P. Y.; Morokuma, K.; Voth, G. A.; Salvador, P.; Dannenberg, J. J.; Zakrzewski, V. G.; Dapprich, S.; Daniels, A. D.; Strain, M. C.; Farkas, O.; Malick, D. K.; Rabuck, A. D.; Raghavachari, K.; Foresman, J. B.; Ortiz, J. V.; Cui, Q.; Baboul, A. G.; Clifford, S.; Cioslowski, J.; Stefanov, B. B.; Liu, G.; Liashenko, A.; Piskorz, P.; Komaromi, I.; Martin, R. L.; Fox, D. J.; Keith, T.; Al-Laham, M. A.; Peng, C. Y.; Nanayakkara, A.; Challacombe, M.; Gill, P. M. W.; Johnson, B.; Chen, W.; Wong, M. W.; Gonzalez, C.; Pople, J. A. *Gaussian 03*; Gaussian, Inc.: Pittsburgh, PA, 2003.
(23) *NIST Chemistry WebBook*; National Institute of Standards and Technology: Gaithersburg, MD, 2001.
(24) Kurnig, I. J.; Scheiner, S. *Int. J. Quantum Chem., Quantum Biol. Symp.* **1987**, *14*, 47.
(25) Hunt, S. W.; Higgins, K. J.; Craddock, M. B.; Brauer, C. S.; Leopold, K. R. *J. Am. Chem. Soc.* **2003**, *125*, 13850.
(26) Yates, B. F.; Schaefer, H. F., III; Lee, T. J.; Rice, J. E. *J. Am. Chem. Soc.* **1988**, *110*, 6327.
(27) Szczesniak, M. M.; Scheiner, S. *J. Chem. Phys.* **1982**, *77*, 4586.
(28) Tuckerman, M. E.; Marx, D.; Klein, M. L.; Parrinello, M. *Science* **1997**, *275*, 817.
(29) Samson, C. C. M.; Klopper, W. *THEOCHEM* **2002**, *586*, 201.
(30) Tuckerman, M. E.; Marx, D.; Parrinello, M. *Nature* **2002**, *417*, 926.
(31) Price, E. A.; Robertson, W. H.; Diken, E. G.; Weddle, G. H.; Johnson, M. A. *Chem. Phys. Lett.* **2002**, *366*, 412.
(32) Robertson, W. H.; Diken, E. G.; Price, E. A.; Shin, J.-W.; Johnson, M. A. *Science* **2003**, *299*, 1367.
(33) Huang, X. C.; Braams, B. J.; Carter, S.; Bowman, J. M. *J. Am. Chem. Soc.* **2004**, *126*, 5042.
(34) Diken, E. G.; Headrick, J. M.; Roscioli, J. R.; Bopp, J. C.; Johnson, M. A. *J. Phys. Chem. A* **2005**, *109*, 1487.
(35) Ayotte, P.; Weddle, G. H.; Kim, J.; Johnson, M. A. *Chem. Phys.* **1998**, *239*, 485.
(36) Chaban, G. M.; Jung, J. O.; Gerber, R. B. *J. Phys. Chem. A* **2000**, *104*, 2772.
(37) Robertson, W. H.; Weddle, G. H.; Kelley, J. A.; Johnson, M. A. *J. Phys. Chem. A* **2002**, *106*, 1205.
(38) Chaudhury, P.; Saha, R.; Bhattacharyya, S. P. *Chem. Phys.* **2001**, *270*, 277.
(39) Lee, H. M.; Kim, D.; Kim, K. S. *J. Chem. Phys.* **2002**, *116*, 5509.
(40) Posey, L. A.; DeLuca, M. J.; Johnson, M. A. *Chem. Phys. Lett.* **1986**, *131*, 170.
(41) Johnson, M. A.; Lineberger, W. C. In *Techniques for the Study of Ion-Molecule Reactions*; Farrar, J. M.; Saunders, W. H., Ed.; Wiley: New York, 1988; Vol. XX, p 591.
(42) Robertson, W. H.; Kelley, J. A.; Johnson, M. A. *Rev. Sci. Instrum.* **2000**, *71*, 4431.
(43) Robertson, W. H.; Price, E. A.; Weber, J. M.; Shin, J.-W.; Weddle, G. H.; Johnson, M. A. *J. Phys. Chem. A* **2003**, *107*, 6527.
(44) Myshakin, E. M.; Sibert, E. L., III; Johnson, M. A.; Jordan, K. D. *J. Chem. Phys.* **2003**, *119*, 10138.
(45) Ayotte, P.; Kelley, J. A.; Nielsen, S. B.; Johnson, M. A. *Chem. Phys. Lett.* **2000**, *316*, 455.
(46) Corcelli, S. A.; Kelley, J. A.; Tully, J. C.; Johnson, M. A. *J. Phys. Chem. A* **2002**, *106*, 4872.
(47) Chipman, D. M.; Bentley, J. *J. Phys. Chem. A* **2005**, *109*, 7418.
(48) McCoy, A. B.; Huang, X.; Carter, S.; Bowman, J. M. *J. Chem. Phys.* **2005**, *123*, 064317.
(49) Bowman, J. M.; Rheineker, J. L. *J. Chem. Phys.* (in press).
(50) Diken, E. G.; Weddle, G. H.; Headrick, J. M.; Weber, J. M.; Johnson, M. A. *J. Phys. Chem. A* **2004**, *108*, 10116.
(51) Hrusak, J.; Friedrichs, H.; Schwarz, H.; Razafinjanahary, H.; Chermette, H. *J. Phys. Chem.* **1996**, *100*, 100.